NASA CR-159612

FIRST SEMI-ANNUAL REPORT

to

NASA-LEWIS LABORATORIES

Energy Conversion and Environmental Systems Division

Grant No. NSG-3169

# EXPERIMENTAL STUDIES OF THE FORMATION/DEPOSITION OF SODIUM SULFATE IN/FROM COMBUSTION GASES

(NASA-CR-159612) EXPERIMENTAL STUDIES OF THE FORMATION/DEPOSITION OF SODIUM SULFATE IN/FROM COMBUSTION GASES Semiannual Report, 16 Nov. 1977 - 15 May 1978 (Yale Univ., New Haven, Conn.) 14 p HC A02/MF A01 CSCL 21B G3/25

N79-25183

Unclas 27128

Principal Investigator: Daniel E. Rosner

Period Covered: November 16, 1977 - May 15, 1978

High Temperature Chemical Reaction Engineering Laboratory

Yale University

Department of Engineering and Applied Science

New Haven, Ct.

## TABLE OF CONTENTS


| Section | Topic | Page |
|---|---|---|
| 1 | INTRODUCTION, MOTIVATION | 1 |
| 2 | BURNER EXPERIMENTS ON DEW POINTS AND DEPOSITION RATE VIA REMOTE OPTICAL METHODS | 2 |
| 3 | H-ATOM ATTACK OF NaCl(s) | 5 |
| 4 | ADMINISTRATIVE INFORMATION | 7 |
| 5 | REFERENCES | 8 |


## LIST OF FIGURES


| | | |
|---|---|---|
| Fig. 2.1 | Arrangement for experimental determination of dew point and salt deposition rates from seeded combustion gases. | 9 |
| Fig. 2.2 | Electrical system for ribbon resistance (temperature) determinations. | 9 |
| Fig. 2.3 | Flat flame burner: constructional details. | 10 |
| Fig. 2.4 | Gas supply/metering system. | 11 |
| Fig. 3.1 | Vacuum flow reactor configuration for studies of Na(g) production *via* the H-atom attack of NaCl(s) surfaces. | 12 |


## LIST OF TABLES


| | | |
|---|---|---|
| Table 3.1 | Na(g) production *via* the H-atom attack of NaCl(s) | 6 |

# 1. INTRODUCTION, MOTIVATION

Gas turbine development is currently being impeded by the severity of high temperature ("hot") corrosion of turbine components resulting from the presence of inorganic salts (e.g. $Na_2SO_4$) in the combustion products [LOWELL et al. (1976); HART and CUTLER (1973)].* While engine operating experience and captive engine tests provide valuable clues to the overall phenomenon, small scale laboratory experiments under more precisely controlled conditions will be essential to cut the cost of future engine design and development based on an understanding of the mechanism of hot corrosion.

The problem can be broken down into a number of important parts, two of which are dealt with in the present program: a) processes governing the availability of sodium for $Na_2SO_4$-formation and b) processes governing the $Na_2SO_4$ deposition rate on surfaces immersed in combustion products. If each of these processes can be understood in detail, it is likely that specific and effective control measures can be identified to suppress the hot-corrosion problem without sacrificing other desirable performance characteristics.

Considering the second problem first (deposition) we note that abundant and precise burner rig deposition rate data are required to develop a successful deposition rate theory relating the laboratory and engine environments [KOHL et al. (1977)]. As a corollary, new experimental techniques are required to acquire such a data base. To date dew points and deposition rates have been inferred from lengthy post-mortem weighings/chemical analysis of platinum foil targets maintained for long periods in laboratory burner rigs intended for materials screening experiments [KOHL et al. (1977), STECURA (1976)].

Second, there is considerable uncertainty about the mechanism and kinetics of $Na_2SO_4$-formation [STEARNS et al. (1977)]. While it is thought that NaCl(c) first vaporizes and its sodium is released via gas phase reactions between the resulting NaCl vapor and atomic hydrogen [cf. e.g. HASTIE (1975)], the kinetics of these "elementary" steps, or rivals to them, have not yet been explored in any detail.

In Sections 2 and 3 specific experiments under well-defined laboratory conditions are described to answer these questions. These experiments, taken together with (i) necessary ancillary data on thermodynamic parameters [KOHL et al. (1975)] (ii) a theoretical framework for predicting dew points and deposition rates [ROSNER (1977), KOHL et al. (1977)], and (iii) follow-on experiments directed at the molecular transport properties of sodium-containing gaseous species, should put the prediction of sulfate formation/deposition phenomena on a much firmer footing.

---

*Similar problems are being encountered in the development of magneto-gas-dynamic energy conversion devices which operate with alkali metal seeds and sulfur-containing fuels (e.g. pulverized coal).

# 2. BURNER EXPERIMENTS ON DEW POINTS AND DEPOSITION RATE VIA REMOTE OPTICAL METHODS*

## 2.1 Background

Precise measurements of dew points, and of deposition rates of inorganic salts formed in combustion product gases, on surfaces exposed to these gases are essential to obtain an improved understanding of the thermochemical and transport processes associated with corrosive salt formation and deposition in gas turbines. Improved measurements would provide data to test the accuracy and domain of validity of the recently developed multicomponent boundary layer theory [ROSNER et al. (1978)], and in the evaluation of future control strategies in efforts to minimize corrosion.

Kohl et al. (1977) have made gravimetric measurements of the deposition rates of sodium sulfate, at atmospheric pressure, on cylindrical platinum targets exposed to the products of a liquid fuel/air combustor. Salt solutions were injected into the combustion chamber through a pump-fed aspirator system. Our purpose is to obtain dew point and deposition rate data of improved precision under better-controlled laboratory conditions. To accomplish this we are exploiting monochromatic laser light to probe condensation onset, and condensate film growth (via interference of reflected light) on electrically heated ribbons immersed in seeded, flat flame combustion product gases. As presently envisioned, the sudden reduction of ribbon heating current would cause a ribbon to radiatively cool through the prevailing dew point, and the condensate onset temperature would be obtained "on the fly". Subsequent deposition rates under these seeding conditions would be obtained from the spacing of intensity maxima in the reflected monochromatic light from liquid condensate films in the submicron (say, $10^{-1}$ to $10^{0}$ μm) range.† To make similar measurements using ellipsometric techniques, a linearly polarized laser has been obtained.

Our strategy is to demonstrate these techniques using a deliberately simple experimental system. Since gases can be more accurately metered into the burner than liquids, we are using boron trichloride as the seed gas in our preliminary experiments. Boric oxide ($B_2O_3$) is formed in such a flame, and the corresponding dew point and deposition rates of this oxide can then be accurately measured by using the abovementioned technique. The results of this set of experiments will be used to demonstrate the proposed experimental techniques and allow us to test the accuracy of chemically frozen boundary layer theory [ROSNER et al. (1978)].

## 2.2 Apparatus

In its present form the apparatus consists of a) an optical system, b) an electrical system for heating the target, and to measure its temperature,

*Prepared by Dr. K. Seshadri

†McIntyre and McTaggart (1970) have used an analogous interference technique to study solid iodide film growth on silver in the submicron thickness range.

c) the burner assembly, and d) gas feed system.

a. Optical System

A schematic illustration of the experimental arrangement is shown in Fig. 2.1. A linearly polarized helium-neon laser (Spectra Physics Model 146P) with an output power level of 4mW is used as a source of monochromatic light. A mirror reflects the laser beam onto the deposition target. The reflected beam from the target is then focussed on the photocell aperture of a photometer (Metrologic Instruments Model 60-230) using two double convex lenses. The photometer output is connected to a strip chart recorder.

The target is a platinum ribbon 50 mm long, 6 mm wide and 0.127 mm thick. The ribbon is held above the burner by two copper rods connected to a d.c. power supply. Two platinum wires of 0.127 mm diameter, were spot-welded across a 4 mm central section of the ribbon. The electrical resistance of this section is calculated from the ratio of the voltage drop across this section of the ribbon to that across a standard resistor in series with the filament.

b. Electrical System

The electrical circuit is shown in Fig. 2.2. The power supply [Kepco model JQE 15-50(M)] can deliver up to 15 v and 50 A at constant voltage or constant current. In constant voltage operation, the output voltage of the power supply can be controlled remotely by an external resistance. The standard resistor is a copper-nickel alloy (Advance 45% Ni).* The ratio of the voltage drop across the central section of the ribbon, to that across the standard resistor is measured on a digital multimeter (Data Precision Series 2000 DMM Model 2500). Since the standard resistor and the platinum ribbon are connected in series the ratio of their voltage drops is equal to the ratio of the electrical resistances; hence the electrical resistance of the ribbon can be calculated from this ratio and the known value of the standard resistance. Since the ribbon electrical resistance depends on its temperature the corresponding temperature is readily calculated.

c. Burner

The burner (Fig. 2.3) consists of a stainless tube A of 25.4 mm inner

*The electrical resistance of this alloy changes negligibly with temperature between 0°C and 100°C (temperature coefficient of resistance is ± 0.000018 Ω/K between 0°C and 100°C). Since the temperature of the standard resistor would never attain 100°C in our experiments, the electrical resistance of the standard resistor can be assumed to be a constant, equal to its value at room temperature, over the entire range of operation.

diameter, and 76.2 mm long welded to a stainless steel plate B. A premixed gaseous stream of fuel, air, and the seed gas is fed to the burner at the bottom of the tube. To obtain a laminar flow of the premixed gases with a uniform velocity above the burner, a porous, monel disk 25.4 mm diameter, and 12.7 mm thick is placed at the top of the tube. The burner is cooled by flowing water through a copper tube fastened to the outer surface of A. A cylindrical copper tube C 50.8 mm inner diameter and 63.5 mm long is attached to tube A. To improve the stability of the flat flame above the burner, and to minimize diffusion of oxygen from the atmosphere into the flame, a flow of nitrogen is maintained through the annular space between tube A and tube C. The annular space between the tubes is packed with glass beads to obtain a smooth flow of nitrogen above the burner. The entire burner assembly is mounted on a base plate D.

d. Gas Feed System

The gas supply (Fig. 2.4) consists of compressed gas cylinders of air, nitrogen, the seed gas (boron trichloride), and the fuel (propane). Variable area flowmeters F1, F2, F3, and F4 (Brooks Instrument Division Sho-Rate "150" Low Flow Indicators), with control valves at outlet, are used to measure the flow rates of these gases. The uncertainties in the measurements are expected to be less than ± 2% of full scale. Since boron trichloride is an extremely toxic, and reactive gas, monel check valves C1, C2, C3, C4, and C5 (Matheson Model 402V) were installed to prevent flow of gases upstream of these valves. Check valves C1 and C3 prevent boron trichloride from contaminating the air and nitrogen lines, check valve C2 prevents air, and nitrogen from entering the boron trichloride line, check valve C4 prevents the fuel from leaking into the flow lines upstream of this valve, and check valve C5 prevents air, and boron trichloride from entering the fuel lines. Stainless steel tubing 6.25 mm diameter, and fittings is used upstream of check valves C3, C1 and C5. The rest of the connections were made with monel tubing of 6.25 mm diameter, and monel fittings. Bourdon-type Gauges G1, G2, G3 and G4 are used to measure the pressure of the gases entering the flowmeters. Boron trichloride is less corrosive in its anhydrous state, but extremely corrosive in presence trace amounts of water vapor. Therefore, it is essential to have the flow lines free from trace amounts of water vapor. The needle valves N1 and N2 are used to purge any water vapor in the flow lines before starting the experiment, and to purge the boron trichloride from the flow lines after the experiment is completed.

## 2.3 Status

During the first semi-annual period the abovementioned system was designed and constructed. Preliminary $B_2O_3$ dew point and deposition rate experiments are now being run, the results of which will be discussed in our second semi-annual report (11/15/78).

# 3. H-ATOM ATTACK OF NaCl(s)*

## 3.1 Introduction

The aim of this phase of our present study is to obtain information on the kinetics and mechanism of the heterogeneous reaction: $H(g) + NaCl(s) \rightarrow Na(g) + HCl(g)$. Because of the importance of gaseous Na(g) as a precursor to $Na_2SO_4(c)$ formation, these data should allow us to evaluate alternatives to mechanisms involving NaCl(c) sublimation.

We are currently carrying out a kinetic and stoichiometric study of this reaction using atomic absorption (AA) spectroscopy combined with microwave discharge-vacuum flow reactor techniques at moderate temperatures. The preliminary results summarized below indicate that H-atom attack of solid NaCl indeed produces Na-atoms, even at surface temperatures as low as at 550°K. At this temperature, NaCl vaporization is negligible, hence the corresponding gas phase (homogeneous) reaction

$$H(g) + NaCl(g) \rightarrow Na(g) + HCl(g) \qquad (1)$$

plays no role in the observed Na(g) production.

## 3.2 Experimental

### Generation of Atomic Hydrogen

Atomic hydrogen streams were produced by passage of a 10% $H_2$, 90% Ar mixture through a microwave discharge cavity [SHAW (1960)]. Ultra high purity grade hydrogen with reported purity of 99.999% $H_2$ (Matheson Gas Company) was used without further treatment. Argon gas with 99.999% purity was passed through an oxisorb cartridge to reduce oxygen content to 5 ppm or less. The H-atom concentration was determined by titration with NO(g) [CLYNE and THRUSH (1962)]

$$H + NO + M \rightarrow HNO^* + M \qquad (1)$$

$$HNO^* \rightarrow HNO + h\nu \qquad (2)$$

The emission intensity I of the HNO* molecules (Reaction 2) is directly proportional to the initial concentration of H atoms, i.e.

$$I = I_o\,[H][NO] \qquad (3)$$

I was measured as a photocurrent mainly due to the $HNO^*(0,0,0) \rightarrow HNO(0,0,0)$ band by using a 0.25 m monochromator with EMI p695 photomultiplier. Kinetic experiments on the H/NaCl(s) reaction were conducted by monitoring atomic hydrogen in argon at about 6 Torr total pressure through the chemical reactor (cf. Fig. 3.1). After the point of discharge, a Teflon [BERG and KLEPPNER (1962)] tube insert is used in the Pyrex system, owing to the very efficient recombination of H atoms on Pyrex.

*Prepared by Dr. P-D. Foo

## NaCl Sample Preparation

Sodium chloride (analytical grade) was melted in a flame and the vapor condensed on a slowly rotating quartz tube with outside diameter 3 mm. A layer of NaCl sample approximately 0.2 mm thick x 4 mm long was used for this study.

## AA Detection of Na Atoms

Sodium atoms produced by the heterogeneous H(g)/NaCl(s) reaction were detected by the atomic absorption (AA) spectroscopy technique. A 0.25 m monochromator at 589 nm was used to monitor the Na(g) absorbance at surface temperatures ranging from about 540 °K to 680 °K. For heating purposes we used a small electrical coil inserted into the sealed quartz-tube that was coated with NaCl sample (see Fig. 1). In our preliminary experiments the temperature of NaCl has been followed using an uncalibrated IR Pyrometer and specimen rotation was not used.

## Preliminary Results and Discussion

Our preliminary results indicate that when sodium chloride is heated to 550 °K or higher and exposed to an atomic hydrogen stream, an appreciable atomic absorption signal at 589 nm appears. The absorption occurs as soon as the heated NaCl is exposed to the atomic hydrogen stream but disappears completely as soon as the atomic hydrogen stream was cut off; either by interrupting the hydrogen gas flow or the turning-off of the microwave discharge. A typical result for the absorbance, A, of Na at 589 nm vs. surface temperature (T) is presented in Table 3.1.

Table 3.1. Na(g) Production via the H-atom Attack of NaCl(s)

| T(K) | $10^3\ T^{-1}\ (K)^{-1}$ | A | ln A |
|---|---|---|---|
| 541 | 1.85 | 0.078 | -2.54 |
| 565 | 1.77 | 0.142 | -1.95 |
| 628 | 1.59 | 0.289 | -1.24 |
| 656 | 1.52 | 0.379 | -0.97 |
| 672 | 1.49 | 0.427 | -0.85 |

By combining the Arrhenius rate expression with the Lambert-Beer Law, one obtains the following relation for the apparent activation energy:

$$E = -R \frac{d\ (\ln A)}{d\ (1/T)} \qquad (4)$$

The data of Table 1 imply an activation energy of about 5.2 Kcal/mole.

Future Work

To obtain absolute reaction efficiencies for the H(g)/NaCl(s) reaction we intend to measure the weight loss of the sodium chloride specimen at various temperatures, upon exposure to atomic hydrogen for known intervals. For this purpose a more complex (detachable, rotatable) heated sample holder is being used. At the same time it may be possible to confirm the stoichiometry of the reaction by quantitatively determining (NO titration) the amount of atomic hydrogen required for the reaction.

## 4. ADMINISTRATIVE INFORMATION

Our work on each of Tasks 1, 2 (optical detection of dew points/deposition rates, and Na(g) release from NaCl(s) via H-atom attack) is progressing well, and no significant "mid-course corrections" appear to be necessary at this point. Task 1 is mainly the work of Dr. K. Seshadri and Task 2 is mainly the work of Dr. P-D. Foo*, both under the general direction of Prof. D.E. Rosner. We anticipate that some of the preliminary results now being obtained on Task 1 can be incorporated into our forthcoming joint Yale-NASA presentation at the NBS conference: Characterization of High Temperature Vapors (September 1978).

In the immediate future we believe a visit of NASA personnel would be fruitful, to discuss our present experimental progress, agree on our emphasis for the remaining six months, and plan for useful extensions of this work which would complement current experimental investigations at NASA-Lewis Laboratories.

Much of the six month progress reported above would not have been possible without the valuable inputs of our HTCRE Laboratory colleagues, especially Drs. P.C. Nordine, B. Halpern and R. Atkins. Their suggestions are gratefully acknowledged here.

*Significant aspects of the AA and flow reactor development have been supported by AFOSR-funds, with some supplementary equipment and consumables funds from the ALCOA Foundation.

## 5. REFERENCES

Berg, H.C. and Kleppner, D. (1962), "Storage Technique for Atomic Hydrogen", Rev. Sci. Inst. 33, 248-249.

Clyne, M.A.A. and Thrush, B.A. (1962), "Mechanism of Chemiluminescent Reactions Involving Nitric Oxide - the H + NO Reaction", Disc. Faraday Soc. 33, 139-148.

Hart, A.B. and Cutler, A.J.B. (1973), Deposition and Corrosion in Gas Turbines, J. Wiley (Halsted Press Book), New York.

Hastie, J.W. (1975), High Temperature Vapors, Academic Press, New York.

Kohl, F.J., Stearns, C.A. and Fryburg, G.C. (1975), "Sodium Sulfate: Vaporization Thermodynamics and Role in Corrosive Flames" in Metal-Slag-Gas Reactions and Processes (Z.A. Foroulis and W.W. Smeltzer eds.), The Electrochem. Soc., Princeton, N.J., 649-664.

Kohl, F.J., Santoro, G.J., Stearns, C.A., Fryburg, G.C. and Rosner, D.E. (1977), "Theoretical and Experimental Studies of the Deposition of $Na_2SO_4$ from Seeded Combustion Gases", NASA TMX-73683 (Technical Paper Presented at the Symposium on Corrosion Problems Involving Volatile Corrosion Products sponsored by the Electrochemical Society, Philadelphia, Pa., May 8-13).

Lowell, C.E., Grisaffe, S.J. and Levine, S.R. (1976), "Toward More Environmentally Resistant Gas Turbines: Progress in NASA-Lewis Programs", NASA TMX-73499 (Technical Paper Presented at the Third Conference on Gas Turbine Materials in a Marine Environment, Bath, England, September 20-23).

McIntyre, R.J. and McTaggart, F.K. (1970), "Comparison of the Reactions of Atomic and Molecular Halogens with Silver", J. Phys. Chem. 74, 866-874.

Rosner, D.E. (1977), "Deposition of Condensible Impurities in Surfaces Immersed in Hot Gases", Semi-Annual Report to NASA-Lewis Laboratories, Grant No. NSG-3107, February 15.

Rosner, D.E., Chen, B.K., Fryburg, G.C. and Kohl, F.J. (1978), "Chemically Frozen Multicomponent Boundary Layer Theory of Salt and/or Ash Deposition Rates from Combustion Gases", submitted for publication in Combustion Science and Technology.

Shaw, T.M. (1960), "Techniques of Electrical Discharge for Radical Production", in Formation and Trapping of Free Radicals, A.M. Bass and H.P. Broida, eds., Academic Press, New York, Ch. 3, 47-67.

Stearns, C.A., Miller, R.A., Kohl, F.J. and Fryburg, G.C. (1977), "Gaseous Sodium Sulfate Formation in Flames and Flowing Gas Environments", Technical Paper Presented at the Symposium on Corrosion Problems Involving Volatile Corrosion Products sponsored by the Electrochem. Soc., Philadelphia, Pa., May 8-13, NASA TMX-73600.

Stecura, S. (1976), "Two-Layer Thermal Barrier Coating for Turbine Airfoils-Furnace and Burner Rig Test Results", NASA TMX-3425.

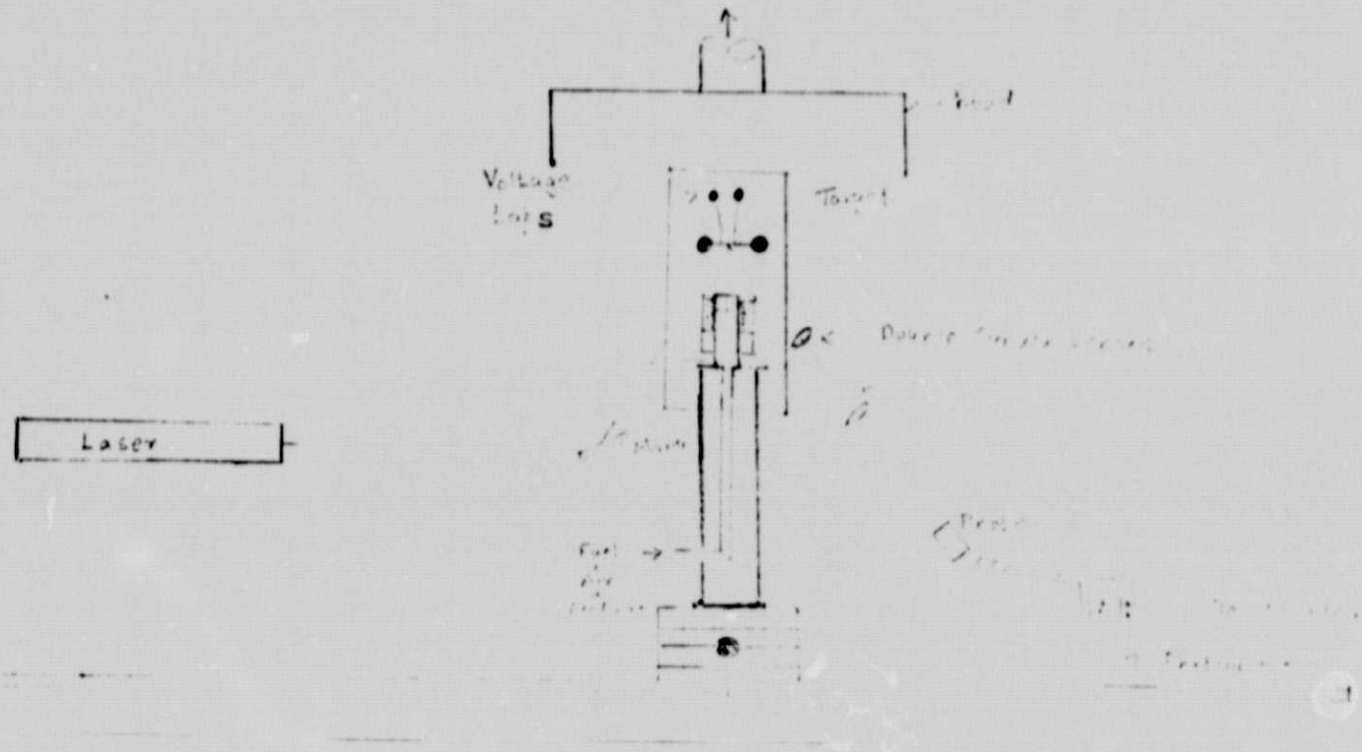


Fig. 2.1. Arrangement for experimental determination of dew point and salt deposition rates from seeded combustion gases.

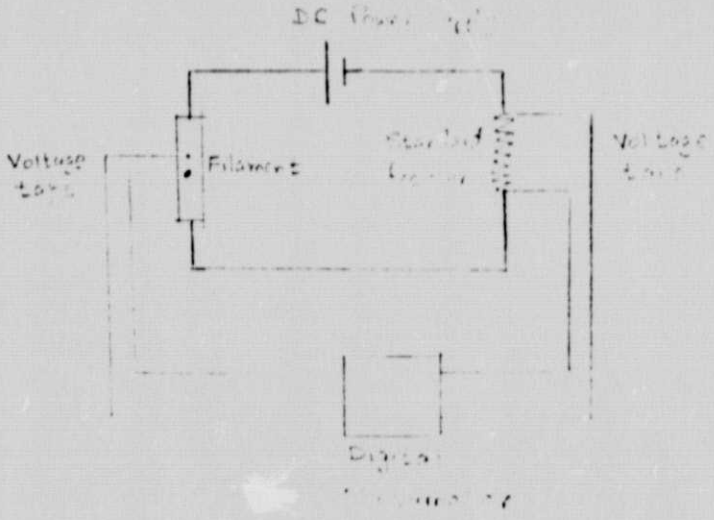


Fig. 2.2. Electrical system for ribbon resistance (temperature) determinations.

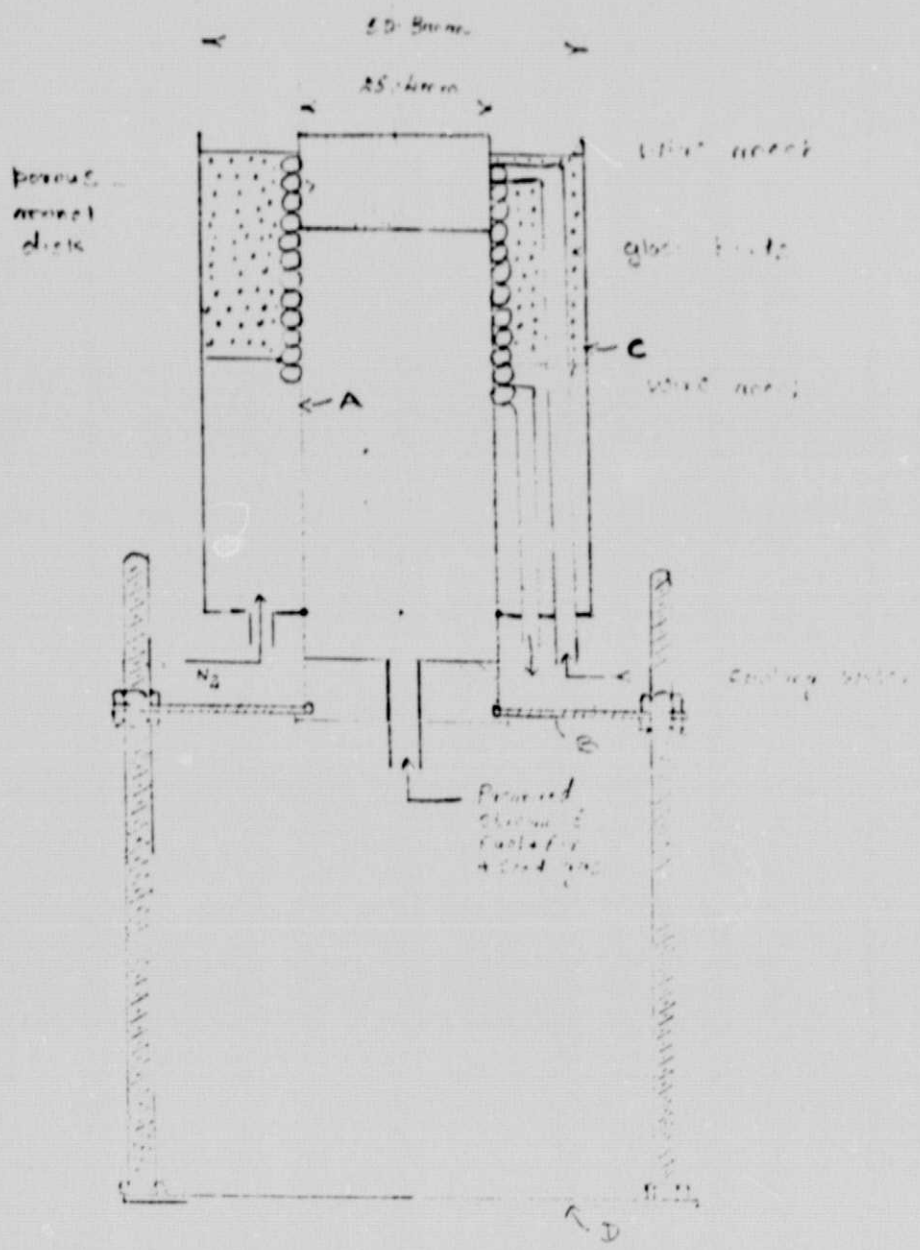


Fig. 2.3. Flat flame burner: constructional details.

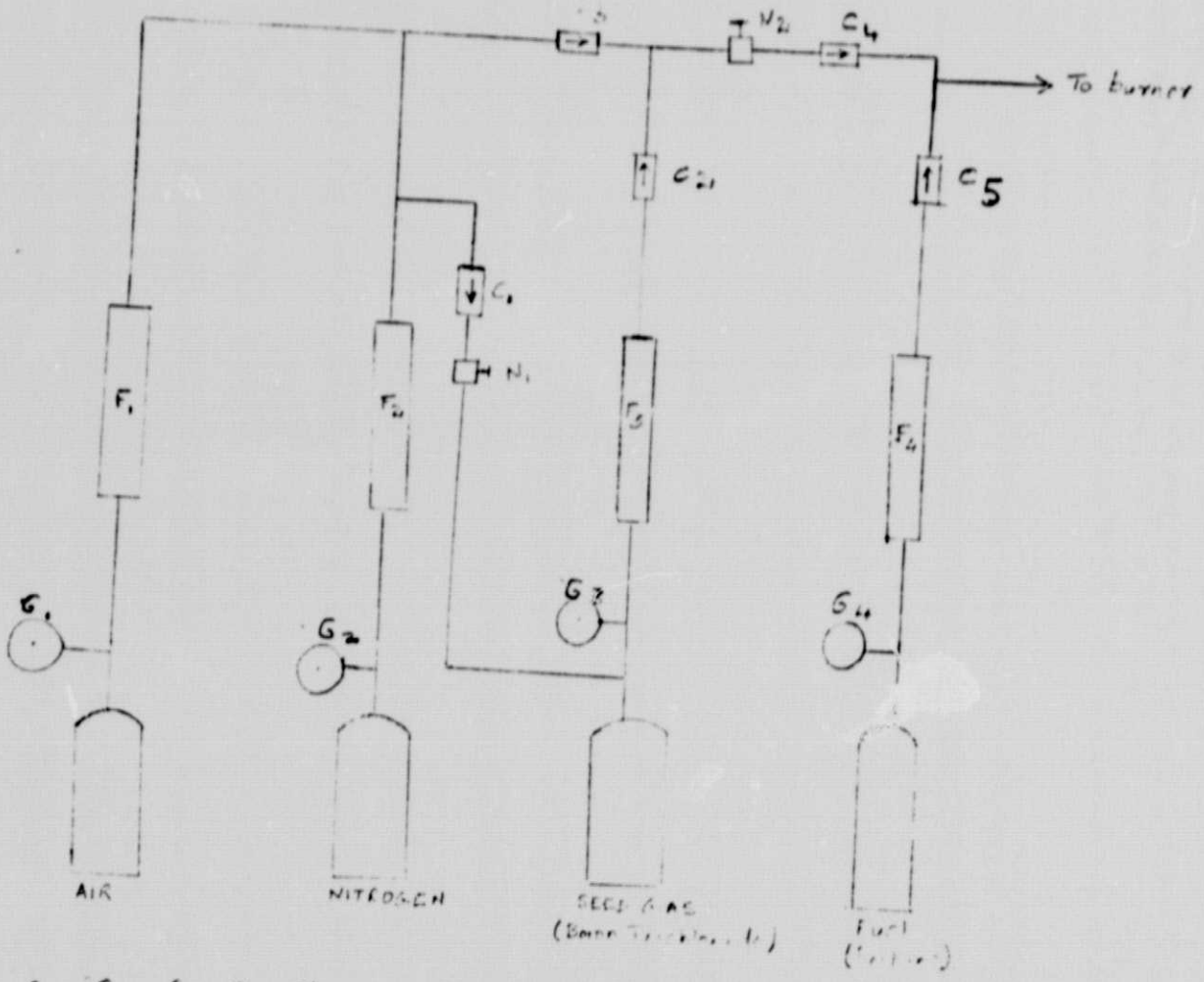


$C_2, C_2, C_3, C_4, C_5$ – check valves.

$F_1, F_2, F_3, F_4$ – Variable [illegible] flow meters

$G_1, G_2, G_3, G_4$ – [illegible]

$N_1, N_2$ – Needle valves

Fig. 2.4. Gas supply/metering system.

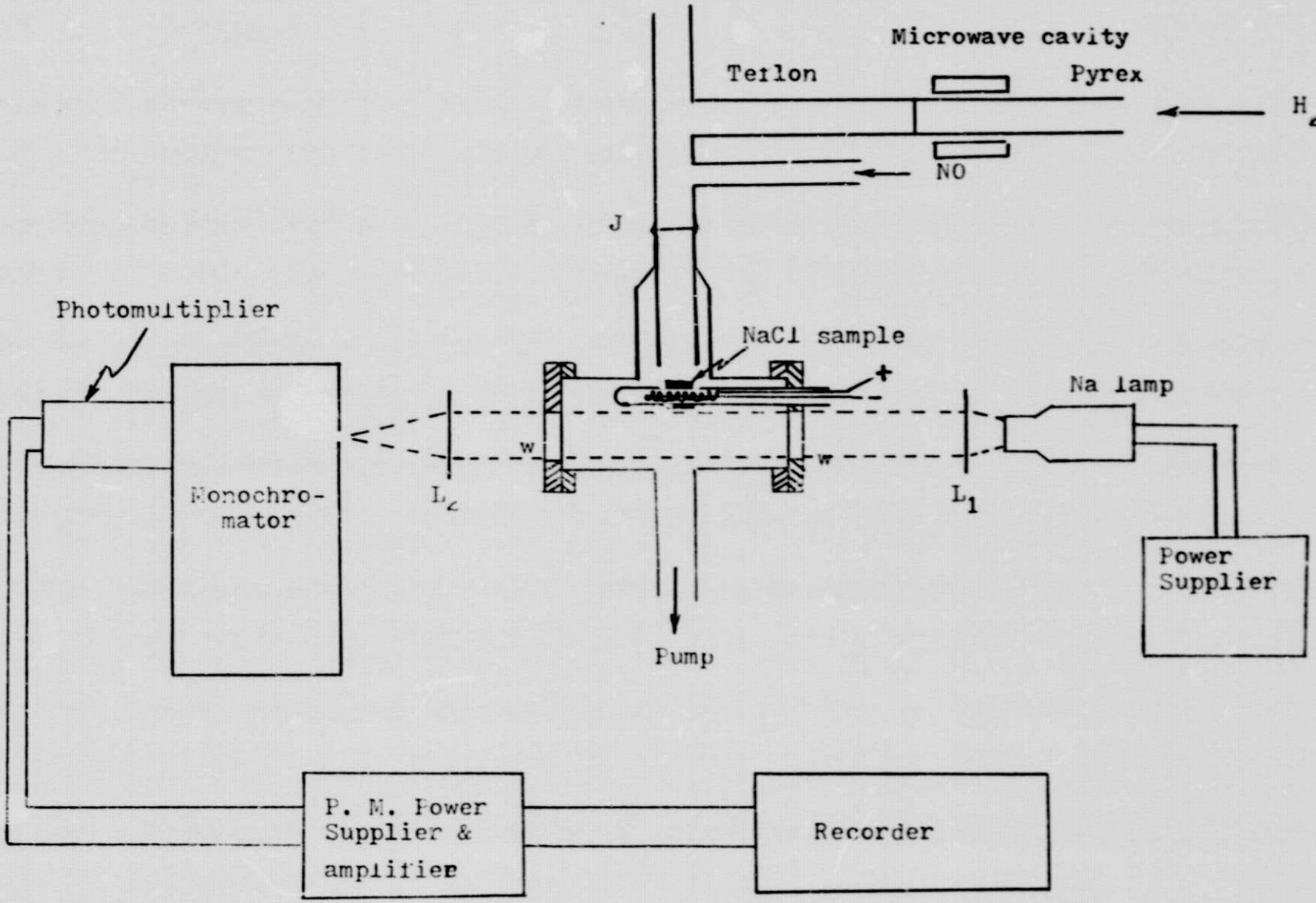


$L_1$, $L_2$ Lens
J, O-ring joint
W, optical window

Fig. 3.1. Vacuum flow reactor configuration for studies of Na(g) production via the H-atom attack of NaCl(s) surfaces.